An Ice Lithography Instrument

Anpan Han 韩安磐[1], John Chervinsky[2], Daniel Branton[3], and J. A. Golovchenko[1,2*]

[1]Department of Physics, Harvard University, Cambridge, MA 02138 USA

[2]School of Engineering and Applied Sciences, Harvard University, Cambridge, MA 02138 USA

[3]Department of Molecular and Cellular Biology, Harvard University, Cambridge, MA 02138 USA

*Corresponding Author. Telephone: 617-495-3905; Email: golovchenko@physics.harvard.edu

Abstract

We describe the design of an instrument that can fully implement a new nano-patterning method called ice lithography, where ice is used as the resist. Water vapor is introduced into a scanning electron microscope (SEM) vacuum chamber above a sample cooled down to 110 K. The vapor condenses, covering the sample with an amorphous layer of ice. To form a lift-off mask, ice is removed by the SEM electron beam (e-beam) guided by an e-beam lithography system. Without breaking vacuum, the sample with the ice mask is then transferred into a metal deposition chamber where metals are deposited by sputtering. The cold sample is then unloaded from the vacuum system and immersed in isopropanol at room temperature. As the ice melts, metal deposited on the ice disperses while the metals deposited on the sample where the ice had been removed by the e-beam remain. The instrument combines a high beam-current thermal field emission SEM fitted with an e-beam lithography system, cryogenic systems, and a high vacuum metal deposition system in a design that optimizes ice lithography for high throughput nanodevice fabrication. The nanoscale capability of the instrument is demonstrated with the fabrication of nanoscale metal lines.

Introduction

An ice resist – for example, frozen water – is particularly attractive for making nano-devices because it is easily vaporized, does not leave a residue, and can be removed without using aggressive organic solvents[1-2]. Although e-beam lithography using organic resists such as poly-methylmethacrylate serves as the backbone tool of many nanoscience laboratories, the process requires several time consuming steps carried out in different machines. More importantly, as demonstrated by electron transport studies of very clean as-grown single walled carbon nanotubes[3-4], optimal device performance is frequently hampered by lift-off residues that contaminate the active nanoscale components. Using ice lithography, we produced pristine single walled carbon nanotube field effect transistors (FET) with good electrical properties without any lift-off contamination[2]. Finally, high resolution, sub 20-nm-wide metal lines that normally require a high-end 100 kV e-beam lithography system can easily be patterned by ice lithography with a modest 30 kV e-beam lithography system.

Our first report on nanopatterning ice with charge particles was carried out using a commercially available focused ion beam and SEM dual-beam system with cryostage and metal sputtering system in the load lock[1]. But we encountered many difficulties inherent in the design of such commercially available cryogenic SEM systems which were developed primarily for biological applications (e.g. Quorum Tech., East Sussex, UK, and Gatan Inc., Pleasanton, CA, USA). Here, we report the design and implementation of an instrument dedicated to ice lithography. Among the most important requirements are the need to (a) have a well focused, high beam current for ice removal; (b) minimize vacuum contaminants and maximize cryogenic shielding to eliminate condensable vapors in the immediate environment of the cold sample; (c) have a system able to coat several different materials normal to the sample surface; (d) accurately measure the thickness of deposited materials; and (e) assure robust cryogenic conditions.

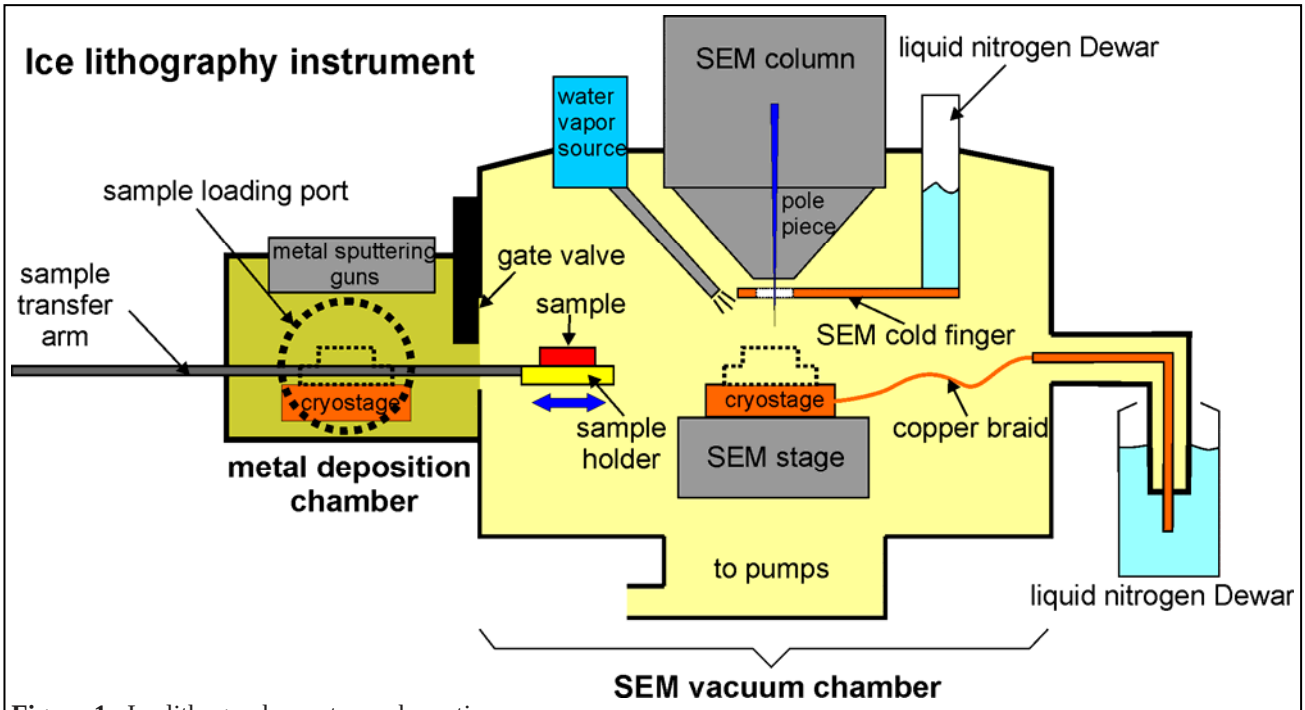

Figure 1. Ice lithography system schematic.

Instrument design

A schematic of the instrument is shown in Fig. 1. It consists of components built into the standard main chamber of a JEOL SEM (model JSM-7001F) and an attached in-house-built metal deposition chamber with transfer arm and sample loading port. Samples that are to undergo ice lithography are placed on the sample holder at room temperature and then loaded into the instrument through the sample loading port on the metal deposition chamber, where the sample holder is attached to the transfer arm. After evacuating the metal deposition chamber, the gate valve to the SEM main chamber is opened. The transfer arm is then used to move the sample holder onto the SEM cryostage, where the sample holder and attached samples are cooled after withdrawing the transfer arm. Components within the SEM main chamber maintain the sample at cryogenic temperatures, shield the sample from vacuum contaminants, introduce and condense water vapor over the sample, map the position of the sample and all of its nano-components, and selectively remove ice in the desired pattern. The transfer arm is then used to withdraw the sample holder and sample into the metal deposition chamber and onto its pre-cooled independent cryostage. After closing the gate valve, metals are dc argon sputter deposited as desired. The metal deposition chamber is then vented with dry N_2 and the sample holder and samples are withdrawn through the metal deposition chamber port. Finally, the samples are

immersed in isopropyl alcohol at room temperature, leaving behind the patterned metal coated regions.

Commercial components of the instrument will be mentioned briefly, while custom designed components will be described in detail. Unless specified, vacuum components and standard feed-throughs were purchased from suppliers Kurt Lesker, Clairton, PA; MDC Vacuum Products, Hayward, CA; Insulator Seal, Sarasota, FL; and VAT Inc., Woburn, MA. Oxygen-free high thermal conductivity (OFHC) copper was used for maximum heat conduction in all cooling components. Four independent temperature controllers (CN77000 series, Omega Engineering, Stamford, CT) measure and regulate the temperature of the cryostages and cold fingers in the SEM and metal deposition chamber, using in-house wired K-type thermocouple sensors (Omega Engineering). For clarity in the 3D illustrations of Fig. 2, most of the electrical connections and cables are not shown.

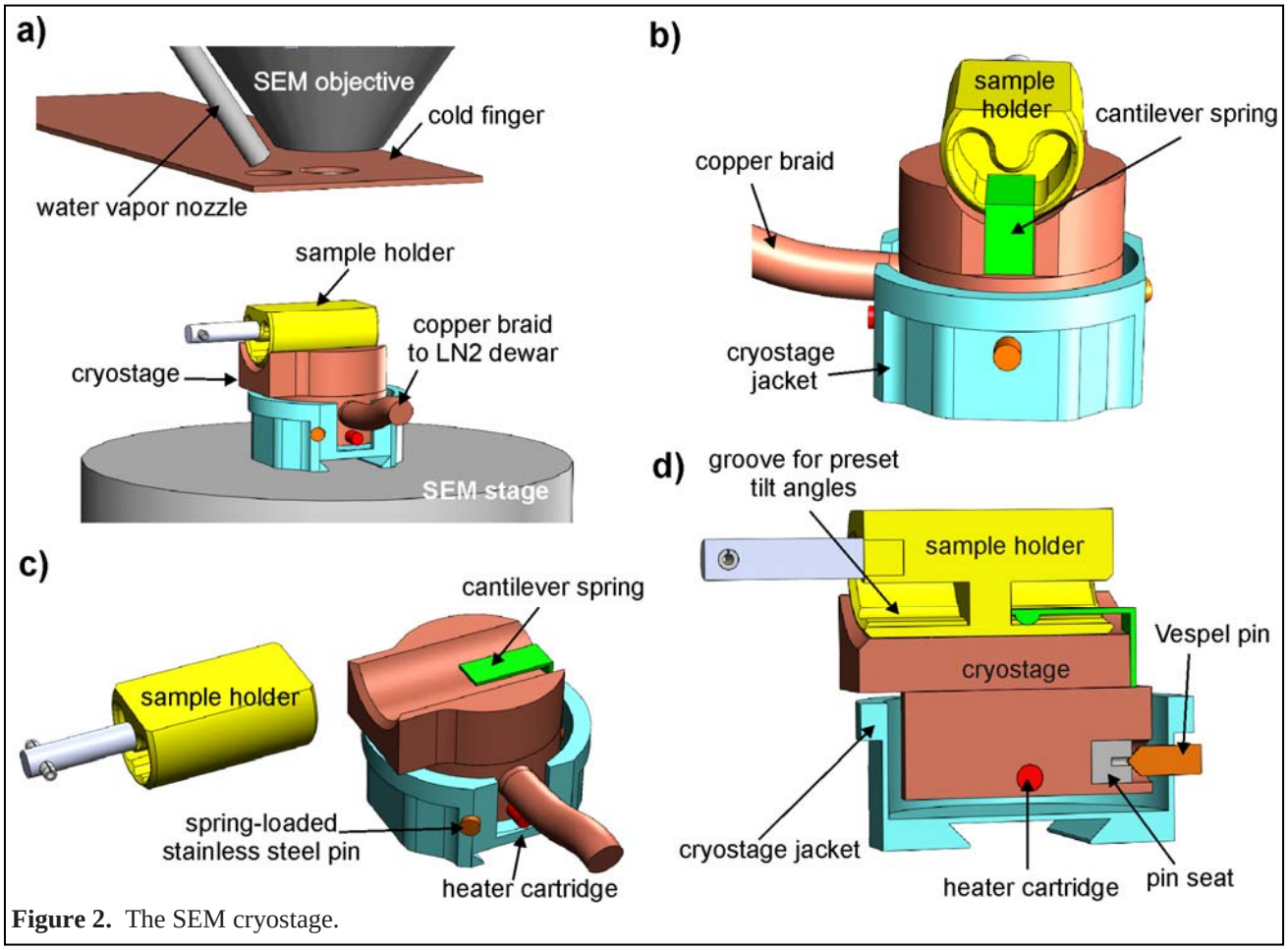

Figure 2. The SEM cryostage.

a. SEM

We selected a JEOL 7001F SEM (JEOL USA, Peabody, MA) as the base for our instrument because it provides a large number of well distributed instrument ports, could be fitted with a robust diffusion pump that evacuates the SEM main chamber, and has a thermal field emission e-beam gun that provides a very stable, well focused high beam current. The 3 nm resolution at 5 nA of beam current is important for ice lithography since the number of electrons required to remove a 100-nm-thick ice layer, also called the clearance dose, is about 10^3-10^4 times the clearance dose needed for a standard Poly(methyl methacrylate) (PMMA)resist[1]. Thus, cold cathode field emission systems with smaller beam currents are poorly suited for ice lithography. To condense volatile gases and improve the SEM chamber vacuum pressure and cleanliness, a liquid nitrogen (LN_2) cooled baffle (JEOL pn: SN-73110) was mounted above the diffusion pump. To monitor gases in the vacuum system and facilitate leak checking operations, a residual gas analyzer (RGA200, Stanford Research Systems, Sunnyvale, CA) was installed in the SEM's main chamber. Because we found that stray magnetic fields in our environment deflected the e-beam and caused visible shifts in the SEM image and e-beam lithography writing patterns, an active magnetic field cancellation system (MK 4 EMI Cancellation System, IDE, Randolph, MA) was installed around the SEM to reduce stray magnetic fields. The stray fields in the bandwidth between 1-1000 Hz were reduced to 0.3 mGauss (root mean square), and the slow drifting fields below 1 Hz varied less than 0.3 mGauss (peak to peak) measured in a time frame of 10 minutes.

The cryostage was built into the standard JEOL 32 mm specimen holder (Fig. 2a), which was re-machined to serve as the cryostage jacket. The cryostage itself consists of a copper base that is cooled by thermal contact through an oxygen-free copper braid (Fig. 2) soldered to the cryostage. The other end of the copper braid was firmly clamped onto a copper rod that was immersed in LN_2 held in an external LN_2 Dewar. To reduce radiative heating, the copper rod and braid were wrapped in aluminized Mylar foil (Rol-Vac LP, Dayville, CT). The cryostage was centered, supported and insulated within the cryostage jacket by two Vespel pins and one spring-loaded stainless steel pin. The pins rest on stainless steel pin seats. Because the only thermal path between the cooled cryostage and the cryostage jacket is through the small contact area of the thermally insulating Vespel pins and stainless-steel pin, the cryostage could be cooled to 110 K while the cryostage jacket remained firmly clamped onto the normal JEOL high

precision stage mechanism at the ambient temperature inside the SEM main chamber. Bearing in mind that the system must maintain the best possible vacuum, direct delivery of LN_2 to the cryostage using flexible Teflon tubing was avoided because Teflon is permeable to helium, making He leak-detection impossible. To minimize re-condensation on the cold sample after the e-beam had removed ice in the desired pattern, a large area LN_2 cooled OFHC copper cold finger shield was mounted directly above the cryostage. OFHC copper was used for the cold finger for two reasons. First, the shield must be non-magnetic, because the shield is in proximity to the electron beam path, and magnetic fields from the shield will perturb the electron beam by Lorentz force, ultimately deteriorate the SEM image. Second, the material must conduct heat well to reach cryogenic temperatures.

Figures 2b and 2c show the cylindrical cavity in the cryostage and how the cylindrical base of the sample holder slides into this cavity. The cross sectional view (Fig. 2d) shows how the cantilever spring secures the sample holder to the cryostage. The cylindrical design of the gold plated cavity and sample holder allows manual sample tilting around the cylinder axis. Tilt angles are preset by grooves machined into the sample holder that seat the cantilever spring.

To control the cryostage temperature above 110 K, a low magnetic field heater cartridge (Sun Electric Heater, Salem, MA) was fitted into the cryostage When in use, the heater caused increased boiling of the LN_2 cooling the cryostage. This made it necessary to isolate the SEM from dewar vibrations caused by the boiling LN_2, which would otherwise impede high resolution SEM imaging and writing. Hence, the heat conducting copper rod used to carry heat away from the braid connected to the cryostage was immersed in a LN_2 Dewar that sat on the floor (Fig. 1), out of contact with the vibration isolated SEM main chamber.

The water vapor nozzle is mounted near the SEM objective, so that one can image and introduce water at the same time. The angle between the water vapor nozzle and the sample is 45º. The water vapor for ice condensation is obtained from a hydrated salt ($MgSO_4.7H_2O$) stored in a quartz tube mounted onto a valve manifold outside the SEM vacuum chamber. Water vapor flow into the SEM chamber is controlled by an ultra high vacuum variable leak valve (pn: 9515106 Varian, Lexington, MA). The valve manifold also contains a pressure gauge tube (275 Convectron Gauges, Granville-Phillips, Longmont, CO) and another valve used to evacuate the vapor above a freshly mounted water vapor source.

After coating a sample with ice, an SEM image of it can be taken to map the location of sample components, such as randomly grown carbon nanotubes, that are to be contacted during ice lithography and metallization. As previously shown, the ice overlaying carbon nanotubes shields the tubes from e-beam induced contamination or damage but does not impede their visualization[2]. Ice is removed from desired contacting electrode regions using an SEM lithography system (NPGS 9, Nabity, Bozeman, MT) and a beam blanker (Deben, Suffolk, UK). After ice removal, an SEM image can be taken to evaluate the quality of the writing, and the sample is then transferred into the metal deposition chamber.

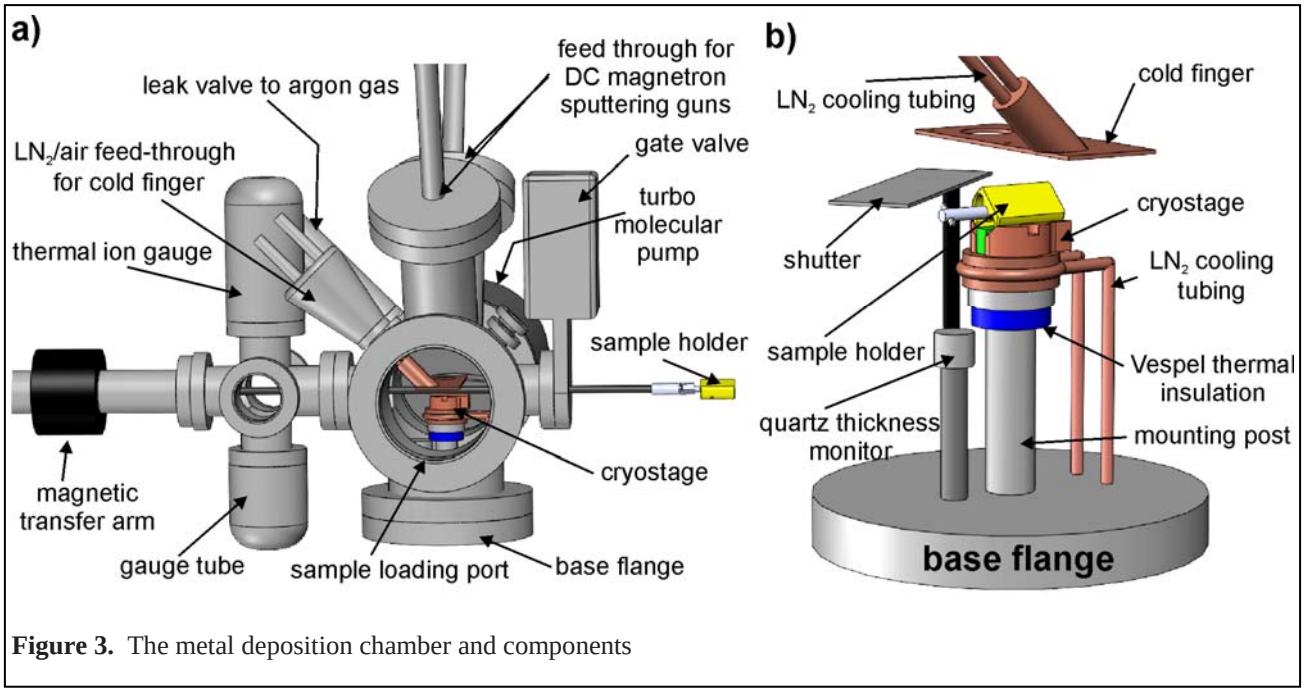

Figure 3. The metal deposition chamber and components

A magnetic high vacuum linear-rotary transfer arm (Huntington, Mountain View, CA) was built into the system to transfer the sample holder between the SEM main chamber and the metal deposition chamber. A transfer arm that translocates any outside air-exposed areas into the vacuum of the metal deposition chamber should be avoided to minimize bringing surface adsorbed water into the vacuum system, where it will condense on the cold sample. The transfer arm is coupled to the sample holder only when the sample holder is to be moved from the SEM main chamber to the metal deposition chamber. Heat flow from the transfer arm to the sample holder during the short time (20 Sec) required to move the sample holder from the SEM main chamber to the metal deposition chamber was minimized by fabricating the male connector on

the sample holder from stainless steel and making the matching female connector on the end of the transfer rod from Vespel.

b. Metal Deposition Chamber

To assure good metal deposition, the vacuum in the metal deposition chamber (Fig.3a) was maintained below 10^{-4} Pa by a 6-inch-diameter low vibration water cooled turbo molecular pump (HiPace 300 from Pfeiffer Vacuum, Asslar, Germany) backed by a rotary pump (Pascal 2010 from Adixen, Hingham, MA, USA) through a vibration isolation unit (JEOL). To keep the overall metal deposition chamber mass low, this water cooled turbo molecular pump was attached directly to the metal deposition chamber without a vibration insulation coupling or a flow regulation valve. The pump's vibration was sufficiently low that it had to be temporarily switched off only when patterning structures with dimensions less than 100 nm.

The metal deposition chamber pressure is monitored by a gauge tube and thermal ion gauge (Granville-Phillips). A logic circuit prevents the pneumatically actuated gate valve (VAT, Inc.) separating the metal deposition chamber from the SEM main chamber from opening prior to establishing a good vacuum in the metal deposition chamber.

Because device fabrication frequently requires two different metals, the metal deposition chamber was fitted with two DC magnetron sputtering guns (1.3" MAK from MeiVac, San Jose, CA controlled by MX 500 Controller from Advanced Energy, Fort Collins, CO) at a 60˚ angle from each other and an ultra high vacuum leak valve (pn: 9515106, Varian, Inc.) to admit high purity Ar for processing.

A standard flat stainless steel vacuum flange, the base flange (Fig. 3b), was modified to serve as the mount for the metal deposition chamber cryostage, associated copper LN_2 cooling tubing and quartz crystal thin-film thickness monitor (STM-2XM, Sycon Instruments, East Syracuse, NY). A manually operated shutter mounted onto a rotary motion feedthrough in this flange (pn: 670000, MDC Vacuum Products, Hayward CA) accurately controls metal deposition. Vespel thermally insulated the cryostage from its stainless steel mounting post (Fig. 3b). An independent LN_2 cooled cold finger was installed just above the metal deposition chamber cryostage.

The gold plated metal deposition chamber cryostage with an *L* shaped cantilever spring that slides into the sample holder mirror-imaged the top portion of the SEM main chamber cryostage (Fig. 2c). The cylindrical design of the gold plated cylindrical cavity and sample holder made it possible to tilt the sample (Fig. 3b). Metals could be deposited normal to the sample plane from both of the sputter deposition units that are separated by 60º. The tilt angles are manually set using the sample transfer rod and grooves machined into the sample holder.

Because the metal deposition chamber cryostage remains stationary and because its vibration requirements are not as stringent as they are for the SEM cryostage, the stage temperature was controlled by directly flowing LN_2 or compressed heated air through copper tubing soldered to the stage. This made it possible to cool or heat the stage very rapidly, greatly shortening total process time because the metal deposition chamber is subject to venting and frosting at the end of each lithography cycle. On the inlet side, a manifold allowed connections to a 160 LN_2 Dewar or compressed optionally heated air. Flows were individually regulated by two manual valves. On the outlet side, the gas is able to leave the circuit via three different exits: a safety pressure relief valve that prevents pressure build up above 1.5 bar; a LN_2 compatible manual valve (Diaphragm-Sealed, Cambridge Valve and Fitting, Billerica, MA) to allow rapid gas or LN_2 flow; and a cryogenic solenoid valve (Gems Sensors & Controls, Plainville, CT). In normal use, one of the CN77000 series temperature controller units senses the cryostage temperature and controls it by the opening and closing of the solenoid valve cooling operations with the inlet LN_2 manual valve open and the manual outlet valve closed. To heat the cryostage quickly, LN_2 flow is stopped by closing the inlet LN_2 manual valve, and compressed warm air is flowed through the circuit. The metal deposition chamber cold finger temperature is controlled by a circuit identical to that for the metal deposition chamber cryostage.

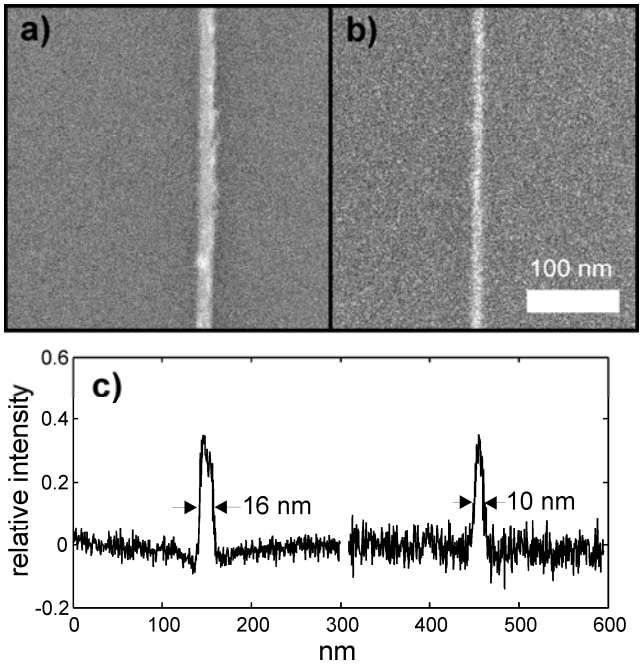

Figure 4. SEM images of metal lines patterned by lift-off. Scale bar is valid for (a) and (b). Line intensity profile (c)..

After the sample is transferred from the SEM to the metal deposition chamber cryostage, Ar is leaked into the metal deposition chamber to serve as the background gas for sputter deposition. The plasma ignited at 1.3 Pa, and the deposition pressure is normally set to 0.40 Pa. The metal deposition chamber is vented to atmosphere using dry nitrogen, and the sample holder is unloaded from the metal deposition chamber cryostage and plunged into isopropanol held at room temperature, which concludes the ice lithography process. (We found isopropanol worked well for lift-off, but have not systematically investigated other reagents.) The metal deposition chamber cryostage and cold finger are then heated to room temperature and are ready for a new sample and ice lithography process.

c. Instrument performance.

Figure 4 shows SEM images of 16 and 10 nm wide metal lines (5-nm-thick palladium) patterned by ice lithography and lift-off. The substrate is a silicon wafer with 300 nm of silicon dioxide that was oxygen plasma cleaned just before insertion in the ice lithography instrument. The ice resist thickness was 20 nm, the beam energy was 30 kV, and the patterning beam current was 150 pA. The line dose was 3 μC/cm for Fig. 4a and 1.8 μC/cm for Fig. 4b. Fig. 4c shows an image intensity profile of a 50 nm wide section perpendicular to the metal lines. These new results are a significant improvement over the 17 nm lines we reported earlier[1] and generally superior to lift-off masks using PMMA. The area doses required to remove an 80 nm layer of ice at respectively 5, 15 and 30 kV are 0.5, 0.9 and 1.0 C/cm^2 as in our previous study[1].

The SEM cold finger is critical to assure that the partial pressure of water vapor near the sample is low, such that undesired ice growth on the sample is negligible during a typical 30 min writing time. Although the JEOL 7001F SEM cannot maintain a vacuum below 7×10^{-5} Pa, the LN_2 cooled baffle and other cold surfaces within the SEM main chamber kept the partial pressure of water in the SEM chamber below 10^{-6} Pa. The SEM cold finger cooled down from room temperature to 83 K in 30 min, and the cold finger Dewar contained sufficient LN_2 for more than 8 hour of care-free operation. The JEOL diffusion pump baffle contained sufficient LN_2 for more than 12 hours of operation. With the partial pressure of water in the SEM chamber below 10^{-6} Pa, less than 20 monolayers of water molecules will grow on an exposed surface at <130 K in 30 min. Since the 83 K SEM cold finger was situated no more than 3 mm away from the sample, the local partial pressure of water in the immediate vicinity of the specimen must be significantly less than 10^{-6} Pa. Our successful lift-offs and metallic line writing lead us to

conclude that the background ice growth must be less than a monolayer in 30 min, which is more than our normal writing time. But for extremely long writing times, >45 min, we did experience problems due to some metal lines incompletely adhering to the sample after it was plunged into isopropanol.

For superior ice lithography, amorphous ice is required. At 10^{-5} Pa, the transition between amorphous and crystalline ice growth occurs at ~135 K. Therefore the cryostage should be held at temperatures below 130 K. Our cryostage cooled from room temperature to 110 K after ~4 hours. The 5 L Dewar for the SEM cryostage easily kept the stage cold for more than 40 h. Immediately after the sample holder at room temperature was transferred onto the cryostage held at 110 K, the cryostage temperature rose to 150 K, but within 20 min. decreased to below 123 K, the temperature at which we typically deposited amorphous water ice. This short cooling time after sample attachment is critical since prolonged cooling could increase the deposition of contaminants onto the exposed sample. In control experiments, the thickness of the deposited ice was determined by writing 800 nm wide lines into the ice down to the substrate. We calibrated the rate at which the thickness of the deposited ice grows for the particular conditions and valve settings used during an ice lithography run by previously having measured the ice thickness following deposition under those same conditions and valve settings. The ice thickness deposited onto the sample was calibrated by the following process. First, we injected an unknown amount of water vapor over the sample and an unknown thickness of ice was deposited. Then we wrote 1-µm-wide lines into the ice followed by raising the cryostage temperature to 163 K. The ice slowly sublimed from the sample surface. We followed the sublimation process by SEM imaging and we measured the increase of width of the initially 1-µm-wide line just before all ice sublimes. Assuming the ice sublimes from all surfaces at the same rate, the line width increase is twice that of the ice thickness. Sampling the ice thickness over an area of 6 by 6 mm with 4 measurements at each corner and one in the center, we found the ice thickness varied by no more than 10%.

For high resolution ice lithography, the performance of the SEM cryostage is critical. Thermally induced mechanical drift and stray magnetic fields from the stage heater can strongly affect the e-beam writing. Because of thermal expansion, any temperature fluctuations will cause the sample to drift mechanically. When e-beam writing was performed at the 110 K steady state temperature, we did not observe such problems. At elevated stage temperatures

these problems are minimized by balancing the constant heat loss to the LN_2 with a low magnetic field heater whose field variations were suppressed by powering it with a constant current from an external low noise DC power supply (Agilent E3617A, Lexington, MA). With this setup, the cryostage temperature variability could be maintained at less than 1 K.

Acknowledgments

The authors thank Dr. Christopher Russo for valuable discussions. We thank Peter Frisella and Ray Aubut for significant engineering contributions to the instrument. Research activities and instrument fabrication were supported by NIH grant HG003703 to J. A. Golovchenko and D. Branton. Dr. Anpan Han was supported by a post-doctoral fellowship from the Carlsberg Foundation, Denmark.

References

[1]G. M. King, G. Schurmann, D. Branton and J. A. Golovchenko, Nano Letters **5**, 1157 (2005).

[2]A. Han, D. Vlassarev, J. Wang, J. A. Golovchenko and D. Branton, Nano Lett. **10**, 5066 (2010).

[3]J. Cao, Q. Wang, D. Wang and H. Dai, Small **1**, 138 (2005).

[4]J. Cao, Q. Wang and H. Dai, Nature Mater. **4**, 745 (2005).

Figure Legends

FIG 1. Ice lithography system schematic.

FIG 2. The SEM cryostage.

FIG 3. The metal deposition chamber and components.

FIG 4. SEM images of metal lines patterned by lift-off. Scale bar is valid for (a) and (b). Line intensity profile (c).